

Surface-enhanced Raman scattering from molecules in tunnel junctions

J. C. Tsang, J. R. Kirtley, T. N. Theis, and S. S. Jha*

IBM T. J. Watson Research Center, P. O. Box 218, Yorktown Heights, New York 10598

(Received 11 May 1981; revised manuscript received 13 January 1982)

Surface-enhanced Raman scattering from molecular monolayers adsorbed at the aluminum oxide—Ag interface of tunnel junctions has been studied as a function of the junction parameters and surface roughness. The surface-plasmon—polariton contribution to surface-enhanced Raman scattering from this system is quantitatively demonstrated in experiments on samples fabricated on holographic diffraction gratings. The existence of a short-range contribution to the surface-enhanced Raman effect is also shown and compared with the predictions of the modulated surface dipole mechanism of Jha, Kirtley, and Tsang.

I. INTRODUCTION

The phenomenon of surface-enhanced Raman scattering has been of considerable interest. While the magnitude of the surface-enhanced Raman effect on a smooth, flat surface remains uncertain, there is no question concerning the existence of a substantial surface-enhanced Raman (SER) effect when certain molecules are in contact with a randomly rough, noble-metal surface in solution¹⁻³ and in vacuum.⁴⁻⁷ The effect has also been observed for molecules adsorbed on discontinuous films and colloids,⁸⁻¹⁰ in metal-insulator-metal tunnel junctions¹¹ and other sandwich structures,¹² and on surfaces with periodic surface structures.^{11,13,14}

We have previously suggested that the large enhancements of the Raman scattering efficiency observed in the doped tunnel junctions arise from both the electrostatics of the roughened metal surface¹¹ and the interaction between the molecule and the metal surface.¹¹ In this paper, we consider in detail the contribution of both effects to the surface-enhanced Raman scattering and obtain quantitative values for the contribution of each to the overall enhancement. This enables us to compare our doped tunnel-junction results with experimental results on other systems and with theoretical treatments of the SER effect. We provide detailed, quantitative results and descriptions of our experimental systems which are lacking in our previous short communications. We show how the various experimental and theoretical effects which we have previously considered separately combine to produce our observed results.

The electrodynamic response of a roughened noble-metal surface is strongly modified by the existence of optically active conduction-electron resonances¹⁵ which produce enhanced electromagnetic fields near the surface.^{16,17} This results in an enhancement of the Raman scattering efficiency of molecules adsorbed on the surface.¹⁶⁻¹⁸ Such a mechanism was first proposed as a cause of SER scattering by Moscovits¹⁷ and demonstrated by Burstein, Chen, and Lundquist⁸ for the localized conduction resonances of an island film and by us and others for the delocalized surface-plasmon—polariton (SPP) resonances of a continuous surface.^{11,19,20} In addition, Chen *et al.*, and others^{18,21-23} pointed out that these surface modes can be excited by the nonradiative near field of an oscillating dipole. If these surface modes are radiative, this provides an additional channel for Raman scattering. Such an effect was experimentally observed by us on grating samples²³ where the two electromagnetic resonances can be separated experimentally. We especially emphasize the diffraction grating results in this paper since they allow us to work with a system where the surface roughness can be characterized, allowing for the detailed comparison of theory and experiment. This is in contrast to most previous work which was done on hard-to-characterize, randomly roughened surfaces. We experimentally show that the resonant excitation of SPP's can produce enhancements of over 2 orders of magnitude in the intensity of Raman scattering from a molecular monolayer adsorbed under Ag in tunnel junctions.

Since the total enhancement of the Raman efficiency of molecular monolayers adsorbed under Ag

films in tunnel junctions can be as large as 6 orders of magnitude, the relatively long-range effects associated with the resonant excitation of the SPP's of our Ag gratings cannot explain the total magnitude of the SER effect. Direct evidence for this comes from Raman spectra obtained on tunneling junctions doped with different molecules. The magnitude of the SER effect depends on the adsorbed molecule. Not all molecules show the same enhancement and different vibrational modes of a given molecule show enhancement factors that differ by 2 orders of magnitude. These results suggest that there are local, short-range contributions to the Raman scattering efficiency which can produce an additional enhancement of 2 to 4 orders of magnitude in our tunnel junctions.

The use of doped, inelastic-electron-tunneling spectroscopy (IETS) junctions in these surface Raman studies allows us to obtain detailed information on the electronic and vibrational properties of the molecular monolayer that is difficult to obtain for the other experimental systems used in SER studies.¹¹ Utilizing the information about the interaction between the Ag conduction electrons and the adsorbed molecules provided by the IETS, we have already introduced a phenomenological model¹⁹ for calculating the short-range contribution to the Raman scattering due to the modulation of the optically induced surface charge density by the molecular vibrations. In contrast to the SPP field enhancement this mechanism only involves the first one or two monolayers. The combination of these two effects quantitatively explains many of our Raman scattering results. Our conclusion on the dual origins of SER scattering from molecular monolayers adsorbed in tunneling junctions is consistent with recent work on SER scattering in both electrochemical cells¹⁻³ and clean metal surfaces in ultrahigh vacuum^{4,5,7,9,13} (UHV) and will be discussed below.

We briefly discuss in Sec. II the solution of Maxwell's equations for the classical electromagnetic field near a submacroscopically rough surface. In Sec. III, we describe the details of our experiments. Our experimental results on the effects of the excitation of SPP's on SER intensity are presented in Sec. IV. In the same section, our results for monolayers in a tunnel junction are compared with SER scattering results in other environments and using other surface topographies. In Sec. V, we consider the additional short-range contribution to the Raman cross sections due to the direct interaction of the adsorbed molecule and the

metal surface. We consider some of the models which have been proposed to explain this short-range enhancement. We show that our results are consistent with the modulated surface charge model of Jha *et al.*¹⁹ We close with a summary of our major results and their bearing on other experiments.

II. THEORETICAL CONSIDERATIONS—ELECTROMAGNETIC EFFECTS

Raman scattering by a molecular vibration occurs through the modulation of the optically induced dipole moment $\mu(\omega)$ by the molecular vibrations. If ω_i is the frequency of the incident radiation and ω_s the scattered frequency, the intensity I_s of the Raman scattering can be written as

$$I_s = \frac{\omega_s^4}{8\pi c^3} \left[\sum_{j=0}^n \left[\delta R_j(-\omega_0) \frac{\partial}{\partial R_j} \right] e_s \mu(\omega_i) \right]^2, \quad (1)$$

where δR_j is the displacement amplitude of the atom j for the mode of frequency ω_0 . The above can always be rewritten as

$$I_s = \frac{\omega_s^4}{8\pi c^3} \left[\sum_{j=0}^n \left[\delta R_j(-\omega_0) \frac{\partial}{\partial R_j} \right] e_s \vec{\alpha}_s \vec{E}_L(\omega_i) \right]^2, \quad (2)$$

where $\vec{\alpha}_s$ is the effective system polarizability and \vec{E}_L is the local electric field seen by the molecule in the medium. Therefore, for a molecular monolayer adsorbed on a metal surface, I_s of a given mode can be modified by changes in the magnitude of the incident field at the molecule due to the presence of the metal surface,^{16-19,21} and by the changes in $\vec{\alpha}_s$ due to the interaction of the molecule with the conduction electrons of the metal.^{19,22,24-26} Since \vec{E}_L is the electric field in the absence of the molecule, $\vec{\alpha}_s$ is an effective polarizability.

For a metal where ϵ_1 , the real part of the dielectric function, is less than -1 , the solutions of Maxwell's equations for a vacuum-metal interface include surface waves which propagate along the metal-vacuum interface but decay exponentially away from the interface both in the metal and in the vacuum. These transverse surface wave solutions are characterized by their tangential wave vector \vec{K}_g ($> \omega/c$) in the plane of the surface.^{27,28} For a flat surface, the SPP's of the metal cannot be

optically excited since the incident light cannot provide tangential wave vectors greater than ω/c . However, if the metal surface shows a periodic profile characterized by a wave vector $\vec{g} = 2\pi/\lambda_g$ where λ_g is the periodicity of the grating, an incident photon with a tangential wave vector $\vec{K}_{i,\parallel}$ in the plane of the surface can exchange momentum with the grating and couple to the SPP wave vector K_g if $\vec{K}_{i,\parallel} + \vec{g} = \vec{K}_g$. Then, for $\epsilon_1 \ll -1$, the optical excitation of this SPP on a metal surface with a sinusoidal profile of amplitude ξ_g and wave vector g produces an electric field E_L at a distance a from the surface, which can be written approximately as¹⁹

$$E_L = 2\xi_g K_g \frac{\epsilon_1^{3/2}}{\epsilon_2} \left\{ \exp \left[-a \left(K_g^2 - \frac{\omega^2}{c^2} \right)^{1/2} \right] \right\} E_i, \quad (3)$$

where ϵ_2 is the imaginary part of the dielectric constant of the metal and E_i is the incident electric field. Equation (3) was obtained in the Rayleigh approximation which is valid when $\xi_g K_g < 1$.¹⁹ Given the optical constants for bulk Ag at 5145 Å ($\epsilon_1 = -11$ and $\epsilon_2 = 0.33$),^{29,30} the grating induced optical excitation of the SPP's of Ag by 5145-Å light on a Ag surface with a shallow $\lambda_g = 8000$ Å, $\xi_g = 200$ Å grating profile can produce a value of E_L over an order of magnitude larger than E_i .¹⁹ The optical excitation of the ideal SPP resonance of an Ag surface with such a grating profile can produce an enhancement of more than 2 orders of magnitude of the Raman scattering efficiency of a molecule near the surface. I_s will depend on the optical constants and the scattering geometry, with the maximum enhancement occurring at the angle of incidence $\theta_i = \theta(\omega_{\text{SPP}})$ where the grating can couple the incident light to the SPP's. These results are similar to the ideal results obtained for the enhancement of the electromagnetic fields above an Ag sphere where the conduction-electron resonances are radiative.^{18,21} We shall consider later the effect of radiation damping and also qualitatively consider the limits of the validity of the Rayleigh approximation when the amplitude becomes large. The presence of the reflected and possible diffracted beams and the nonresonant excitation of the conduction-electron modes of the surface will produce a small additional enhancement of the local field. Such an enhancement of about 3 was obtained by Wang *et al.*¹⁸ in their calculations on a sphere. On our grating surfaces, these nonresonant contributions to the enhancement of the Raman scattering will be less than an order of

magnitude. Our ability to make detailed calculations for the grating structures justifies the experimental study of samples fabricated on grating substrates.

The intensity of the Raman scattering from a grating should also depend on the scattering angle θ_s . The adsorbed molecule can inelastically scatter a SPP into another surface-plasmon polariton.¹⁶ The grating momentum is then necessary to couple the scattered SPP to light. This effect involves both the modification (renormalization) of the free space molecular polarizability α by the metal surface and the coupling out to light of the scattered field through the polarization of the metal. Aravind, Hood, and Metiu²² suggest that the Raman enhancement due to the resonance in θ_s will be weaker than the enhancement due to the resonance in θ_i . This is similar to the behavior observed by Chen *et al.*¹⁶ for the prism coupling of light to the SPP's of a thin Ag film. In this regard, our periodic surfaces behave differently from the small sphere systems^{18,21} where the enhancement of the scattered field through the polarization of the sphere is equal to the enhancement of the local field at the sphere surface. Although the E_L enhancement of I_s will be larger for the sphere, the grating surface has the advantage that it is possible to experimentally separate the resonances in θ_i and θ_s by controlling the scattering geometry. This allows an independent measurement of each effect.

As pointed out, these calculations are appropriate when $\xi_g K_g \ll 1$. When $\xi_g K_g \cong 1$, corrections to Eq. (8) include the radiative damping of the surface mode.³¹ For large values of ξ_g , E_L will not increase linearly with ξ_g but will saturate.³¹

The above results where we only consider the electrodynamics for the resonant excitation of SPP's will describe the behavior of a system in the limit where the electronic wave functions of the molecule and the metal surface have no significant overlap. This will not be the case for the first molecular monolayer on a metal surface where one expects significant overlap between the electrons of the molecules and the metal surface. There are a number of possible short-range effects and we shall consider the modification of the optically induced charge distribution at the metal surface by the adsorbed molecule in Sec. V.

III. EXPERIMENTAL DETAILS

The experimental work in this paper was performed on doped metal-insulator-metal tunnel junctions prepared in the same way as samples

used for IETS studies.^{32,33} The samples were doped with either carboxaldehydes or carboxylic acids such as benzoic acid, nitrobenzoic acid, 4-pyridine carboxaldehyde, 4-acetylbenzoic acid, using either ethanol or water as the solvent. Metals used for the overlayer included Ag, Au, Pb, Cu, Sn, and Al.

The IETS spectra of these junctions show the presence of a single, chemisorbed layer at the oxide surface. No scattering from the 1700-cm⁻¹ vibration of the C=O bond of either the COH or COOH groups of the free molecule is observed in IETS.³² In contrast, scattering from the symmetric and asymmetric (1380 and 1550 cm⁻¹) vibrations of the COO⁻ group bonding to the oxide surface is observed.³² The IETS also provides us with information which helps to characterize the electronic properties of the molecule-metal interface.³³ These properties can be important in determining the Raman scattering process.

A model for the electronic structure of an IETS junction is shown in Fig. 1. Both the oxide layer and the molecular monolayer are approximated by barrier potentials for conduction electrons in the left and right electrodes. Korman *et al.*³³ have extracted the value of Φ_{b2} , the molecule-metal barrier potential, from the current-voltage characteristic. They find it can vary between a fraction of an eV and 4 to 5 eV. The IETS spectra of our samples were obtained at either 4.2 or 2 K using a current modulation produced by a voltage modulation with an amplitude between 1 and 5 mV. The second derivative of the current-voltage relationship for the junction was obtained by sensing the second-harmonic voltage signal due to the current modulations.³²

The quantitative characterization of the surface roughness necessary for SER scattering has been a

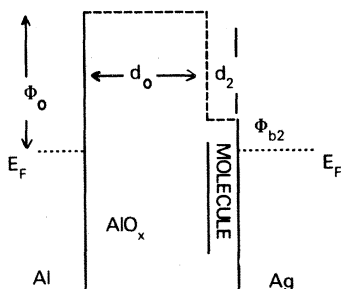


FIG. 1. Model of the electronic structure of a metal-insulator-molecule-metal tunnel junction (from Ref. 33). d_0 and d_2 are the thicknesses of the oxide and the molecular layers. Φ_0 and Φ_{b2} are the barrier heights at the Al-oxide and Ag-molecule interfaces.

major problem for the understanding of the SER effect. In our experiments, the roughness was provided in a controlled fashion through the preparation of the substrate on which the thin-film junction was deposited.

Two different types of substrate roughness were used. The simplest involved the evaporation of CaF₂ onto the microscope slide.¹⁵ This introduces surface roughness whose rms amplitude ξ increases with increasing CaF₂ thickness.³⁴ All of the CaF₂ thicknesses in this paper are average thicknesses based on the mass deposited on a quartz crystal monitor positioned next to the substrate in the evaporator.

Surface structures with a single dominant Fourier component were also introduced into our tunnel junctions by depositing them onto the sinusoidally undulating surfaces of holographic diffraction gratings and the triangular profiles of ruled gratings. The grating surfaces could be quantitatively characterized with just two or three parameters. The ruled gratings were blazed 600, 1200, and 1800 line/mm gratings. Electron micrographs showed that the groove profiles were triangular with amplitudes of the order of several thousand angstroms. The holographic gratings were fabricated using the 3250-Å line of a He-Cd laser.³⁵ The hologram from this laser exposed a 5000-Å layer of photoresist spun on a Si substrate. The amplitude of the grating and the groove profile could be varied by controlling the exposure and development of the photoresist.³⁵ In Fig. 2, we show an electron micrograph of one of these gratings after a doped Al-AlO_x-Ag junction was fabricated on it. The white line at the bottom of the picture shows the junction in profile. The top half of Fig. 2 shows the surface of the grating at normal incidence. The grating has a smoothly varying, almost sinusoidal, profile. Fluctuations with correlation lengths small compared to the grating periodicity can be observed on the surface of the grating but their amplitude is too low to be seen in the grating profile.

Tunnel junctions fabricated on these gratings showed strong coupling between light incident on the junction and the SPP's of the junction²³ including a sharp minimum in the reflectivity for *p*-polarized light at the appropriate value of θ_i .^{15,23,27} We have previously reported that Ag-AlO_x-Al tunnel junctions fabricated on holographic diffraction gratings can produce *p*-polarized SPP emission in the visible when biased above 2.0 eV.³⁶ Similar emission peaks are observed from our doped junc-

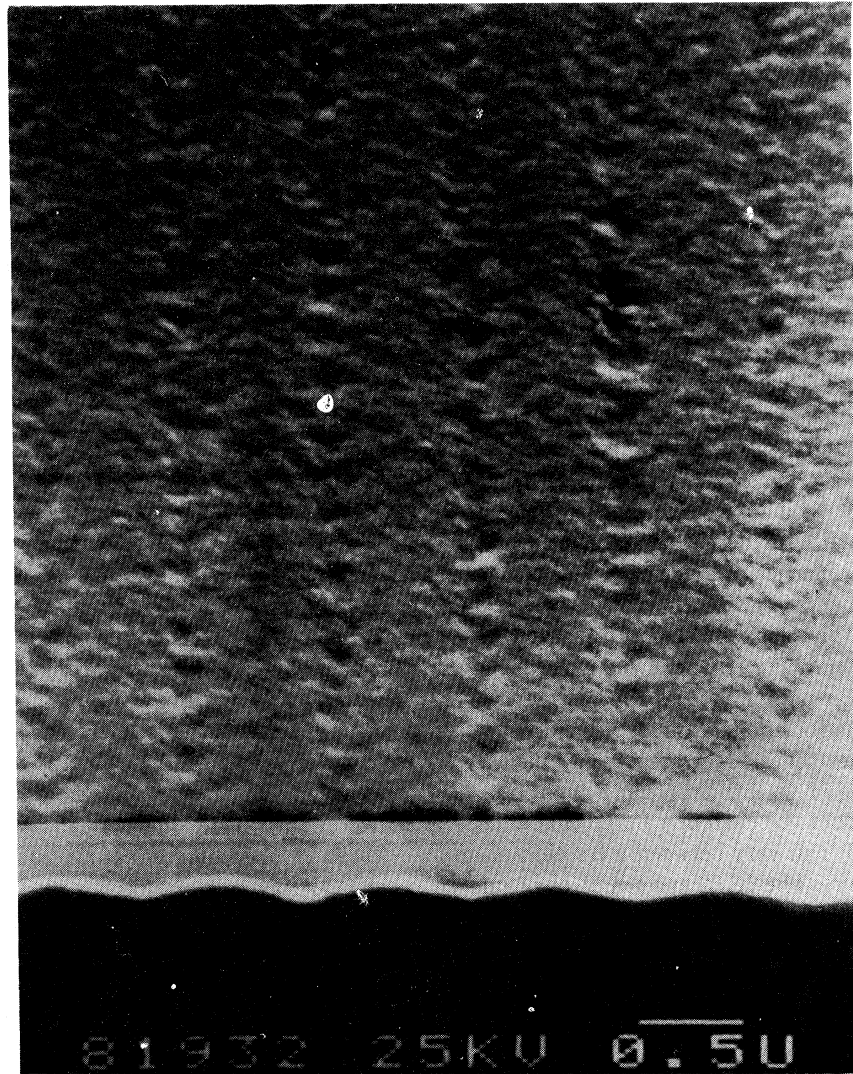


FIG. 2. Electron micrograph of an Al-AlO_x-Ag tunnel junction laid down on a holographic diffraction pattern developed in photoresist. Top is at normal incidence. White line at bottom is junction in profile.

tions.^{23,26}

All of our experiments were performed with the discrete lines of either an Ar⁺ or Kr⁺ laser. Measurements were made in air and at 2 K in liquid He. The scattered light was collected by an *f*1.5 lens and analyzed by a double monochromator with photon counting detection. In some measurements, the collection angle θ_m was deliberately reduced by the placement of an aperture before the collecting lens. This allowed us to study the dependence of the scattering intensity on θ_s . A number of different scattering geometries were employed. The relevant experimental parameters in these measurements are shown in Fig. 3.

IV. EXPERIMENTAL RESULTS— SURFACE-PLASMON-POLARITON EFFECTS

In Sec. II, we showed that an electromagnetic field incident on a metal surface with a sinusoidal profile, could, when $\vec{K}_{i,\parallel} + \vec{g} = \vec{K}_g$, excite the surface electromagnetic waves of the metal. The resultant enhancement of E_L produces a large enhancement of any Raman process involving molecules at the surface. The excitation of these SPP's by the scattered field of the molecule should produce a further enhancement of the Raman efficiency.

We quantitatively test these theoretical results by

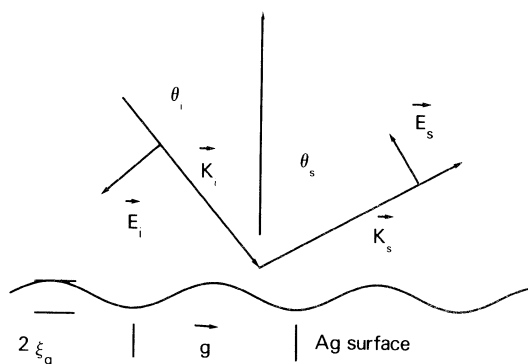


FIG. 3. Experimental parameters for surface-enhanced Raman studies on a metal surface laid down on a diffraction grating.

studying the Raman scattering from doped Al-AlO_x-Ag junctions laid down on holographic gratings with a periodicity of 8000 Å and 100 Å ξ_g <math>< 1200</math> Å. In curve *a* of Fig. 4, we show the Raman spectrum of such a junction doped with 4-pyridine carboxylic acid and excited by *p*-polarized

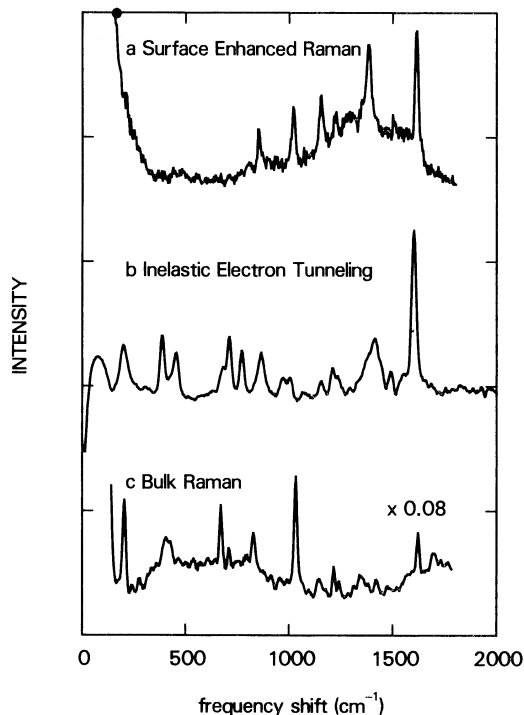


FIG. 4. Vibrational spectra of 4-pyridine carboxylic acid as seen in curve *a* surface-enhanced Raman scattering from a doped Al-AlO_x-Ag tunnel junction on an 8000-Å periodicity grating, curve *b* the IETS spectrum of a doped junction, and curve *c* Raman scattering from a pressed pellet.

light incident at $\theta(\omega_{\text{SPP}})$. $\vec{k}_i \times \vec{g}$ is parallel to the grating grooves. In curve *b* of Fig. 4, we show the IETS spectrum of 4-pyridine carboxylic acid in an Al-AlO_x-Ag tunnel junction held at 2 K. In curve *c* of Fig. 4, we show the Raman spectrum of 4-pyridine carboxylic acid obtained from a pressed pellet of reagent grade power. Both curves *b* and *c* have been processed to remove broad continuum backgrounds.

Both infrared and Raman-active modes of the adsorbed molecule are observed in the IETS of the junction. A comparison of curves *b* and *c* in Fig. 4 with the published infrared spectrum of the acid shows that with the exception of the disappearance of certain modes associated with the COOH group, which dissociates on the oxide,³² there are no significant changes ($< 25\text{ cm}^{-1}$) in the vibrational frequencies of the 4-pyridine carboxylic acid molecule when it is adsorbed at the metal-oxide interface and covered by a thin film of Ag. A comparison of the SER spectrum in curve *a* and the IETS spectrum in curve *b* of Fig. 4 suggests that these two spectra also arise from the same molecules. While not all the lines seen in the IETS spectrum are seen in the Raman spectrum, all of the lines in the Raman spectrum have close counterparts in the IETS spectrum.

The broad band observed in the IETS data at 1380 cm^{-1} arises from the COO group bonded to the oxide surface.³² It has been shown that this is the only species present.³⁷ The observation of a similar broad band in the SER spectrum shows that the molecules observed in our SER spectra are chemically bonded to the oxide and are part of the surface monolayer. We shall make a more detailed comparison of the Raman, IETS, and SER spectra in Sec. V. In this section, we first consider the magnitude of the SER effect in our junctions and the contribution of the SPP excitations to this magnitude.

The 1594-cm^{-1} C-C ring mode of the pressed pellet in curve *c* of Fig. 4 is between 2 and 5 times more intense than the same mode in the doped junction on a grating with a 1000-Å amplitude (Fig. 4, curve *a*). The saturation surface density n_s of the pyridine carboxylic acid molecules is $7 \times 10^{14}\text{ molecules/cm}^2$.³⁷ The number of molecules per unit volume of pyridine carboxylic acid n_v is about $5 \times 10^{21}\text{ cm}^{-3}$. The Raman spectrum of the translucent pressed pellet was excited with the same optics used in the tunnel-junction SER measurements. The ratio of the bulk and the surface scattering depends only on the scattering

length l . l is determined by θ_i on the pellet and the projection of the slit width of the monochromator on the sample. The comparative number of molecules excited in the tunnel junction and in the pellet is $n_s/n_v l$. We measure $l=200+100\ \mu\text{m}$. There are approximately 10^5 more molecules in the scattering volume of the pellet than in the scattering area of the junction. The Raman scattering efficiency of the 1594-cm^{-1} mode for the monolayer on a grating is approximately 5×10^4 greater than that of the molecules in the pellet assuming that all the molecules at the junction contribute equally to I_s . The corrections associated with the finite thickness of the Ag layer will be introduced later. The enhancement factor of 5×10^4 is not the same for all scattering geometries and for all lines in the SER spectrum of the molecule. The surface enhancement of the 3061-cm^{-1} C-H vibration (not shown in Fig. 4) is at least a factor of 100 less than the enhancement of the 1594-cm^{-1} mode. Comparison of curve *a* of Fig. 4 with the experimental results of Kuiper *et al.*³⁸ on benzaldehyde adsorbed on alumina shows that the changes in the relative intensities of different lines in Fig. 4 do not arise from the chemisorption of the molecule on the oxide surface.

Measurements of the Raman spectrum of the doped oxide before the evaporation of the Ag overlayer and of regions of the doped oxide away from the Al- AlO_x -Ag junction show no evidence of Raman scattering from the 4-pyridine carboxylic acid dopant. Given our experimental sensitivity, any enhancement factor associated with the SPP resonances of the Al substrate and the presence of more than one layer of molecules on the oxide must be much less than 500. The enhancement of the Raman intensity of the Al surface due to the excitation of the Al SPP fields will be almost 2 orders of magnitude weaker than the enhancement of the Raman scattering on the Ag [Eq. (3)].²⁹ The failure to observe any scattering from the molecular monolayer on AlO_x -Al shows therefore that the observable SER effect in our junctions depends on the presence of the Ag overlayer.

We have observed strong signals from experimental systems using underlayers other than the Al- AlO_x layer used in Fig. 4. These included Ag, CaF_2 ,¹² and Mg- MgO_x . In the first two cases, the observed signals were over an order of magnitude stronger than in our Al- AlO_x tunnel junctions. However, IETS measurements were generally not possible on these samples so we could not independently verify the presence of a single molecular

monolayer. Therefore, we will not pursue these results further in this paper.

If doped tunnel junctions with 200-Å or thicker Ag films were fabricated on nominally smooth microscope slides, the SER spectra were either unobservable or barely observable. In the latter case, the scattered intensity varied from spot to spot. Observable signals were often obtained from spots showing strong elastic scattering suggesting the presence of roughness in the junction due to impurities, dirt particles, etc.

The SPP contribution to I_s for molecules adsorbed in a tunnel junction laid down on a grating should vary as ξ_g^2 [Eqs. (2) and (3)]. In Fig. 5, we show this for a nitrobenzoic acid-doped junction. In this experiment $\theta_i = \theta(\omega_{\text{SPP}})$. The data were obtained by translating the excitation along a sample with a variable-amplitude grating profile. The amplitude was measured by a scanning electron microscope. These results resemble those obtained in other systems where the SER signal increases with increasing roughness.³⁹ However, the interpretation of all of these results is somewhat uncertain since the measurements are made either on different samples or different regions of the same sample. This raises the possibility of contributions from other surface-dependent effects. The study of the SPP contribution to SER scattering from a

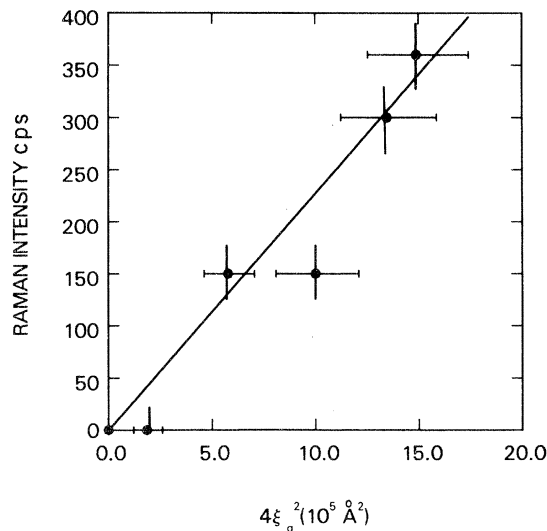


FIG. 5. Dependence of the intensity of the 1594-cm^{-1} line of 4-nitrobenzoic acid in an Al- AlO_x -Ag tunnel junction on the square of the amplitude of the 8000-Å periodicity sinusoidal grating used as the substrate. The Raman spectrum was resonantly excited by pumping the surface-plasmon-polariton absorption of the ing.

grating can, however, also take place on a single sample or spot on the sample. The coupling between the light and the SPP field shown in Fig. 5 to vary as ξ_g^2 also varies with θ_i and θ_s .

Figure 6 shows the SER spectra of a nitrobenzoic acid-doped tunnel junction for different values of θ_i and θ_s and *p*-polarized incident light. These spectra were obtained using an optical collection angle, $\theta_m = 30^\circ$. I_s varies strongly with θ_i and θ_s , but we observe no significant change in the relative intensities of the Raman lines or their energies with either angles. This is expected from Eq. (2) and a θ_i -dependent enhancement mechanism which involves the enhanced E_L 's but does not effect the Raman polarizability tensor.

We also observe broad bands in the spectra in Fig. 6. Unlike the Raman lines from the molecular vibrations, the energies of these bands are determined by θ_s and are independent of the excitation energy as seen from a comparison of curves *b* and *d* in Fig. 6. Their intensities depend strongly on θ_i in the same manner as the intensities of the Raman lines. These broad bands have also been observed in undoped junctions and on thick Ag films laid down on gratings. We have previously reported

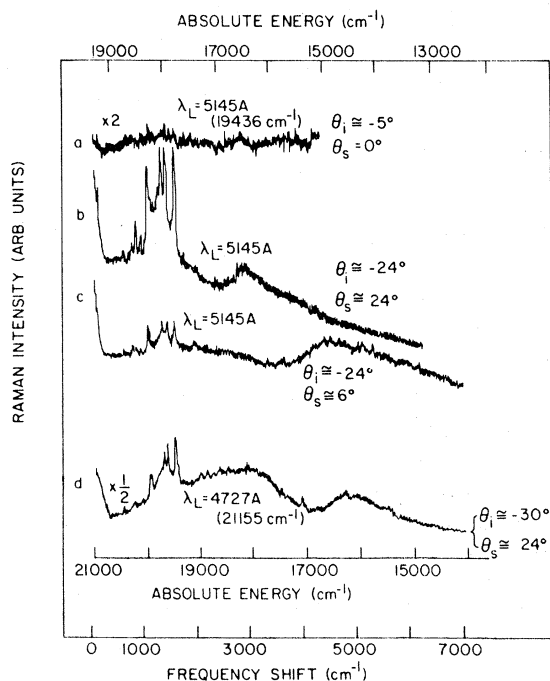


FIG. 6. Raman spectra of an Al-AlO_x-Ag tunnel junction doped with nitrobenzoic acid and fabricated on an 8000-Å periodicity sinusoidal diffraction grating. The different spectra correspond to different scattering geometries and excitation wavelengths. The energy scale for spectrum *d* is just below the trace.

angle-dependent, optical emission from an undoped Al-AlO_x-Ag tunnel junction laid down on an 8000-Å grating and biased at 2.5 eV which is similar to the broad bands in Fig. 6.³⁶ The quantitative differences in the linewidths of the bands in Fig. 6 and Ref. 36 arise solely from the different acceptance angles used in the two experiments.

The emission band in Fig. 6 arises from the coupling of optically excited SPP's to light through the roughness of the grating.⁴⁰ In Fig. 7, we show the dispersion curve obtained from this optically pumped emission. The observed dispersion curve shows that the optical emission involves the SPP's of our Ag films. It shows that the optically excited SPP's produce Stokes shifted surface plasmon polaritons which can decay into photons with an efficiency comparable to the efficiency of the SER process for molecules such as nitrobenzoic acid.²³ Figure 6 suggests that such a process will make a substantial contribution to the structureless continuum observed in SER studies on randomly roughened surfaces. A more detailed discussion of this emission is to be found in Ref. 36.

We have previously presented the dependence of I_s from a nitrobenzoic acid-doped Al-AlO_x-Ag junction on θ_i and θ_s for *p*-polarized incident light.²³ We find that I_s from a typical sample can vary by a factor of at least 200 with changes in θ_i and θ_s . If we fix $\theta_s = 0^\circ$ so that for finite θ_i , we can have only a single resonance condition satis-

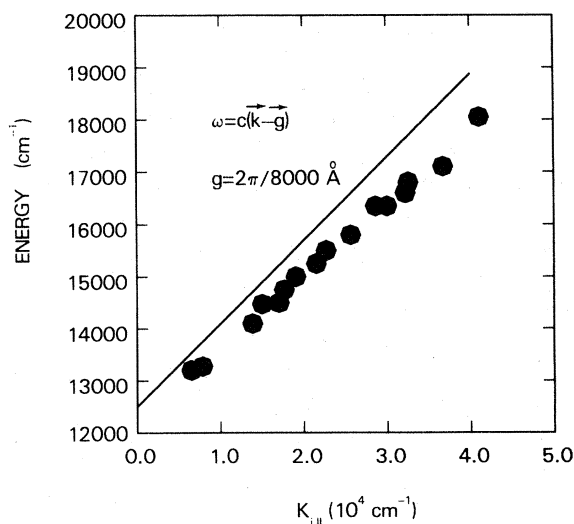


FIG. 7. Dependence on the optical momentum in the grating plane of the energy of the broad, angle-tunable emission observed from optically pumped, Ag tunnel junctions fabricated on an 8000-Å periodicity sinusoidal diffraction grating. The solid line represents the light line shifted by one reciprocal-lattice vector.

fied, we observe a factor of 50 change in intensity with θ_i .

The angular dependence of the SER scattering from molecules adsorbed in a tunnel junction laid down on a grating is similar to the predictions of Chen *et al.*¹⁶ for molecular Raman scattering via the prism coupling of light to the SPP's of a metal film. This is especially true with regard to the weakness of the dependence on θ_s as compared to θ_i . These results point out the principal advantage of using a diffraction grating for these SER studies. The grating system allows the explicit separation of the enhancement of the scattering efficiency by the enhancement of the incident field and the enhancement of the scattering efficiency by the polarization of the metal surface by the scattered Raman field. These results support the recognition by Jha *et al.*¹⁹ that a dominant electromagnetic contribution to the SER scattering from a simple grating surface for $\xi_g K_g < 1$, involves the excitation of the SPP's by the incident beam.

In Fig. 8, we show the dependence of the SER scattering on the polarization of the incident beam and the grating orientation for junctions fabricated on a grating. The SPP effects are observed for *p*-polarized light when the grating wave vector and the projection of the optical wave vector in the grating plane are colinear. The spectra in Fig. 8 were obtained for $\theta_i = \theta(\omega_{\text{SPP}})$ using a 4-pyridine carboxylic acid-doped Al-AlO_x-Ag tunnel junction laid down on a commercial 1200 line/mm diffraction grating. Curve *a* shows the Raman spectra for *p*-polarized incident light, a grating orientation where $\vec{g} \times \vec{K}_i$ is parallel to the grating grooves, and *p*-polarized scattered light. Curve *b* shows the Raman spectrum for the same scattering geometry excited with *s*-polarized light. Curve *c* shows the Raman spectrum obtained with *p*-polarized light and with the grating rotated by 90° so that $\vec{K}_i \times \vec{g}$ is in the plane of incidence. The alignment errors are of the order of 3–4°. Figure 8 shows that strong Raman scattering is only observed when the SPP's of the junction can be directly excited by the incident light.

All of our results on gratings show weak Raman scattering for geometries where neither the incident nor scattered light couple to the SPP's of the film through a first-order interaction with the grating. This can be seen by comparing curve *a* of Fig. 6 where θ_i and θ_s are off resonance and curve *b* where both angles are at resonance. The electron micrographs of this grating surface show the presence of small scale random roughness similar to

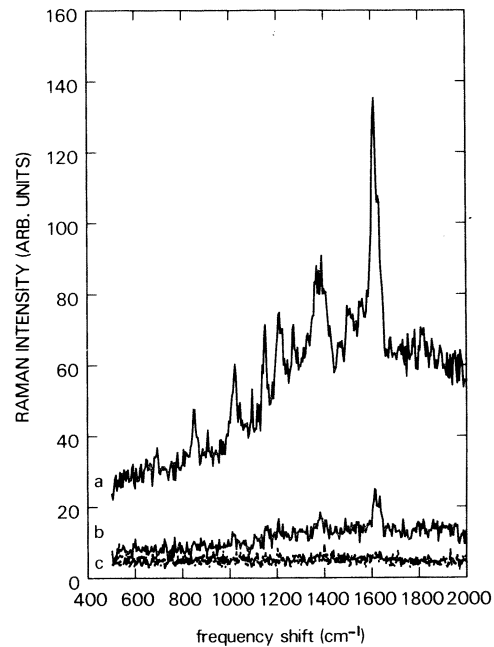


FIG. 8. Surface-enhanced Raman spectra of an Al-AlO_x-Ag tunnel junction doped with 4-pyridine carboxylic acid and laid down on an 1200-Å periodicity, blazed, diffraction grating. *a*, Raman spectra excited by *p*-polarized incident light at the photon-surface-plasmon-polariton resonance condition. *b*, Raman spectrum excited by *s*-polarized incident light using the identical scattering geometry as above. *c*, Raman spectrum excited by *p*-polarized light using the same scattering geometry as above only with the grating oriented so that $\vec{g} \times \vec{k}_i$ is in the plane of incidence.

that in Fig. 2. It is well known that randomly roughened Ag surfaces can show surface-enhanced Raman scattering.

We will now consider the quantitative contribution to the SER effect of one type of random roughness to obtain an appreciation for the scale of random roughness required to produce observable SER scattering. Random roughness with a correlation length G of between 500 and 1000 Å can be obtained from the deposition of Al or Ag films onto previously evaporated CaF₂.³⁴ We have shown (Ref. 11) the SER spectrum of a 4-pyridine carboxylic acid-doped Ag junction of CaF₂. This spectrum is identical to the spectrum shown in Fig. 4. The change in correlation length from the 8000 Å of the grating to the 500–1000 Å of the CaF₂ does not effect the relative intensities of the Raman lines.¹¹

Endriz and Spicer³⁴ observed that the surface-plasmon absorption of Ag films laid down on CaF₂

increases monotonically with ξ , saturating for $\xi \gg 1000$ Å. Analogous behavior was observed by McCarthy and Lambe in their studies of the light emission excited by inelastic tunneling (LEIT) in Al-AlO_x-Ag films laid down on varying thicknesses of CaF₂.⁴¹ We have previously compared the dependence on CaF₂ film thickness of the intensity of the LEIT and the SER scattering. Both show a similar functional dependence on ξ . The intensity of both SER scattering and LEIT saturate for CaF₂ thicknesses above 1000 Å. Laks and Mills³¹ showed that while the roughness induced coupling of the light to the SPP varies as ξ^2 , the surface plasmons can be damped, for large values of ξ , by the radiative coupling. This damping increases with ξ so that for large values of ξ , the strength of the coupling to light will be independent of ξ . We indicated in Sec. II that similar behavior was to be expected from our grating samples for large ξ_g . We have compared the intensity of the roughness-induced, short-correlation-length SER scattering with the intensity of the grating-induced SER scattering for a 1000-Å thick CaF₂ film and a $2\xi_g = 1200$ -Å grating with an 8000-Å periodicity. We find that the peak Raman intensities agree within a factor of 3. Since the intensity of the SPP coupling to the short-correlation-length roughness is proportional to ξ^2 , the residual scattering which we observe away from the SPP resonance condition would be consistent with the presence of surface roughness with $\xi = 5$ Å. This amount of roughness is not unexpected given the sample profile shown in Fig. 2. It is consistent with our observation that the intensity of the residual Raman scattering varies greatly from sample to sample and from spot to spot. The presence of random roughness can provide a background level of enhanced Raman scattering. In this case, our grating-induced, angle-dependent effects can be considerably larger than the experimentally observed values, since the off-resonance signals can arise from the coupling of light to the SPP's through the residual roughness.

All of the results presented in this paper were obtained on samples with the dopant molecules located at the oxide-Ag interface under a 200-Å layer of Ag. Corrections must be made for finite ξ_g and the actual optical properties of the Al-AlO_x-Ag layers if we are to compare our results with our simple theoretical model¹⁹ and with the results obtained in other experiments where the molecules are adsorbed onto a surface.¹⁻¹⁴

Equation (3) was obtained using the Rayleigh

approximation. This approximation is rigorously valid for sinusoidal gratings when $\xi_g K_g < 0.448$.⁴²⁻⁴⁴ Experimentally, the approximation is valid for $\xi_g K_g$ as large as 1 for sinusoidal profiles.⁴⁴ However, it has been found experimentally that expressions such as Eq. (3) cannot be applied to Ag gratings when $\xi_g K_g > 0.2$.^{42,45} This is due to the radiative damping of the SPP's by the grating.⁴⁵ The enhancement of E_L due to the optical excitation of the SPP's will saturate for values of $\xi_g K_g > 0.2$, or in our case of 8000-Å periodicity gratings, for peak to peak amplitudes in excess of 600 Å.

Our measurements of the optical emission from either optically pumped or tunneling electron pumped SPP's allow us to put an upper limit on the magnitude of ϵ_2 of our films. The real part of the dielectric constant is relatively insensitive to the details of the sample preparation so we can use the published values. At 2.3 eV, we have measured SPP emission full widths at half maximum of about 60 meV. If this linewidth were completely attributed to the Ag dielectric losses, it would correspond to a value of $\epsilon_2 = 1.2$.¹⁹ If we assume that for this sample, the dielectric losses are somewhat greater than the radiative losses,⁴⁵ then we obtain a value of $\epsilon_2 = 0.7$ which is consistent with the measurements of Dujardin and Theye.³⁰ This would result in an enhancement of I_s for an adsorbed molecule on a 600-Å amplitude grating of about 200. While further increases in the ξ_g would produce an additional enhancement, the rate of increase would be considerably slower than the ξ_g^2 dependence observed for smaller grating amplitudes. The enhancement of the Raman scattering intensity due to the optical excitation of the SPP's will be between 200 and 300. Since the presence of a metal surface under a molecule will produce a factor of 2-4 enhancement of the Raman scattering due to the reflection of the incident beam, the variation of I_s on our grating with θ_i will be between 50 and 150.

The finite thickness of the Ag overlap and the presence of the molecular monolayer at the oxide-Ag interface means that corrections also have to be made for the optical screening introduced by the Ag layer. In Fig. 9, we show the dependence on the Ag film thickness of the intensity of the 1598-cm⁻¹ line of nitrobenzoic acid adsorbed in Al-AlO_x-Ag tunnel junctions laid down on CaF₂. There is an initial increase in the SER intensity because (1) $\epsilon(\omega)$ is a strong function of the thickness for very thin films and (2) the films do not become

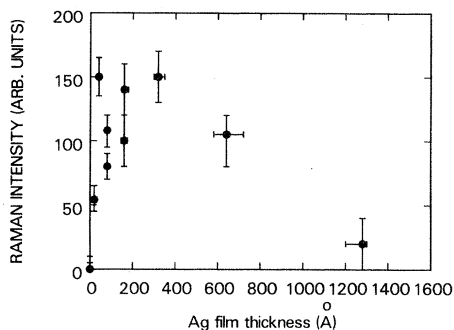


FIG. 9. Dependence on the Ag film thickness of the intensity of the SER scattering from nitrobenzoic acid-doped Al-AlO_x-Ag tunnel junctions fabricated on CaF₂. The thicknesses are mass thicknesses obtained from a quartz microbalance.

continuous until their average thickness is over 100 Å. For average thicknesses below 100 Å, the film consists of small isolated balls of Ag. Since the excitation of the localized modes of the discontinuous film produces a substantial enhancement of I_s ,^{18,21} changes in I_s will occur as the film structure changes. It is interesting to note, however, that I_s for the discontinuous films on our rough substrates is comparable to that of our continuous films. The rapid decrease in I_s with increasing Ag thickness for thicknesses above 200 Å is due to the attenuation of the electromagnetic fields as they pass through the Ag film. In Fig. 10, we show that the Raman spectrum of chemisorbed nitrobenzoic acid on AlO_x does not depend on the thickness of the Ag layer. Since the very thin layers involve surface topologies consisting of random arrays of microscopic Ag particles, this shows that the transition from the small particle resonances to our extended SPP resonances does not change the relative intensities of the Raman lines.

Calculations of the SPP fields in an Al-AlO_x-Ag structure show that their penetration depths into the metal are of the order of 100 Å. Therefore, the intensity of the SPP field under a 200-Å layer of Ag will be about 20% of its intensity at the top of the film. The optical transmission in the visible of a 200-Å-thick film has also been measured. It can be about 20% for films similar to those used by us. I_s is attenuated by over an order of magnitude because of the finite thickness of the Ag layer. This correction will be only weakly dependent on scattering geometry. As a result, the enhancement factors we obtain experimentally are at least an order of magnitude smaller than the enhancement factors before attenuation. Therefore,

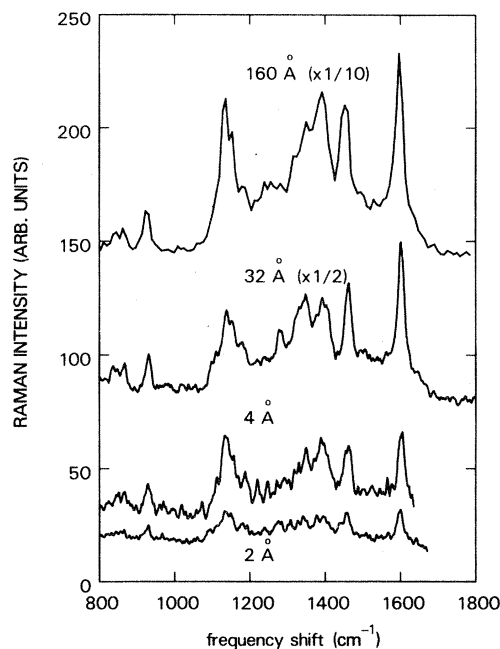


FIG. 10. Surface-enhanced Raman spectrum of nitrobenzoic acid adsorbed on CaF₂-Al-AlO_x and covered by 2, 4, 32, and 160 Å of Ag. The Ag thickness is the mass thickness obtained from a quartz crystal microbalance.

the Raman scattering efficiency of 4-pyridine carboxylic acid adsorbed on Ag, under the resonant excitation of the SPP's of the Ag substrate (Fig. 4), can be almost 10⁶ larger than the scattering efficiency of the same molecules in a pellet. This enhancement factor is close to the factors that have been reported in electrochemical cell experiments.

With these considerations, we can quantitatively compare our experimental results on 100–1200-Å amplitude, 8000-Å periodicity, grating substrates with our calculations for Raman scattering from a monolayer on an Ag surface with a sinusoidal profile. While we have not calculated the enhancement of the Raman scattering due to the molecule-induced polarization of the metal, we can neglect this contribution when $\theta_s = 0$ where the SPP's excited by the scattered field cannot couple to light. When $\theta_s = 0^\circ$ the experimentally observed factor of 50 or more change in the Raman intensity with θ_i is smaller than the 50–150 we would expect. However, we have previously shown that the measured angular variation of the Raman enhancement can underestimate the grating-induced SPP contribution to the enhancement due to the presence of random surface roughness which

can induce measurable SER scattering at nominally nonresonant angles.

While we can understand the θ_i dependence of I_s in our doped junction, it is also clear that the resonant excitation of SPP's cannot explain the full magnitude of our experimentally observed effect even at $\theta_s=0$. We find that the observed enhancement is over 3 orders of magnitude stronger than calculated. The difference between our experimental enhancements and our calculated enhancements is close to the differences we observe between the enhancement factors for different Raman lines of a given molecule and to the differences we observe for the enhancement factors for different molecules. For example, if we consider the 3061-cm^{-1} C-H vibration of 4-pyridine carboxylic acid adsorbed on the grating, we find from the tunneling spectrum that the mode remains well defined in the junction but that any surface enhancement must be less than 10^3 . We will consider detailed evidence for this behavior in the next section of this paper and show that it probably reflects changes in the Raman tensor $d\alpha_s/dR_j$.

If the excitation of SPP's can play an important role in SER scattering from molecules adsorbed under Ag, similar results should be obtainable for molecules adsorbed under other noble metals. This will be true if the excitation energies are in the red where the SPP excitations are well defined in Cu and Au.²⁹ We have fabricated tunnel junctions doped with molecules such as nitrobenzoic acid using Cu and Au counter electrodes. Although we were unable to measure the IETS spectra of these samples, we were able to observe SER scattering. The intensity of the Au spectrum is approximately 50 times weaker than the Ag spectrum. Given $\epsilon(\omega)$ of Au and Ag at 6471 \AA and Eq. (3) the field enhancement in Au should produce a Raman enhancement about 20 times weaker than that produced by Ag.

We have attempted to observe SER scattering from tunnel junctions doped with 4-pyridine carboxylic acid or nitrobenzoic acid and fabricated with counter electrodes of Pb, In, and Sn. None of these metals support well-defined SPP's in the visible. The IETS spectra of the dopant under the Pb counter electrodes show the dopant at the interface. In none of these cases were we able to observe SER scattering. This suggests that the absence of surface electromagnetic wave excitations makes the observation of SER scattering very difficult. Given our requirement of a minimum enhancement of 500, however, these results do not imply that there is no

enhancement of I_s of the molecules, but that any enhancement is less than 500.

The similarities between our results and those obtained in electrochemical cells, discontinuous films, and ultrahigh-vacuum experiments suggest that similar phenomena are observed in all the experiments. The electrochemical cell results of Furtak and Kester⁴⁶ for the quantitative dependence of the SER intensity on the magnitude of the substrate dielectric function and the results of many groups¹⁰ on the SER effect for pyridine adsorbed onto Ag colloids show experimentally that the excitation of the electromagnetic wave resonances can produce an enhancement of at least 2 orders of magnitude of the Raman scattering efficiency. On the other hand, the observation^{47,48} of the infrared-active, Raman-inactive modes of pyrazine on Ag shows that the electrochemical cell results involve fundamental changes in the Raman tensor itself. The large enhancements observed by Chen and Burstein²¹ for Raman scattering from discontinuous films doped with carboxylic acids and carboxaldehydes have been identified with the excitation of the electromagnetic resonances of the small particles which make up the film. The striking differences⁸ between the SER spectra of Ag films laid down on benzoic acid monolayers and benzoic acid monolayers laid down on Ag films, however, show that local effects are important in this system also.

Finally, a number of experimental results on roughened surfaces in ultrahigh vacuum have shown the existence of a long-range, electromagnetic field contribution to the SER effect.^{7,13} However, most of the UHV experiments have also shown the presence of a short-range, local contribution to the SER effect.^{4,6,9,13} These experiments find that the enhancement of I_s from the first monolayer is stronger than any enhancement of the scattering from the subsequent adsorbed layers. Experiments involving roughness introduced at 300 K show short-range contributions to the enhancement of between 10 and 100, i.e., comparable to the extra enhancement we need to explain our results.

V. THE EFFECT OF AN Ag SURFACE ON THE RAMAN POLARIZABILITY $d\alpha_s/dR_j$

The molecule and mode-dependent effects we have observed in our junctions appear to be similar to the short-range effects observed in SER experiments in UHV and related to the extra enhance-

ment needed to explain our intensities. In this section, we make explicit these relationships by comparing the IETS spectra with the SER spectra and also show that the additional molecule-dependent enhancement in our tunnel-junction samples is a short-range, local effect. We then consider some of the models that can explain the presence of this short-range effect.

In Fig. 11, we show the Raman spectra of Al-AIO_x-Ag tunnel junctions laid down on 1200 Å of CaF₂ and doped with 4-pyridine carboxylic acid. Both spectra were excited by 5308-Å light. Curve *a* was obtained at 300 K with no bias voltage applied to the junction while curve *b* was obtained at 2 K with 0.5-V bias applied to the junction. Curve *b* therefore corresponds to the exact experimental conditions for the IETS measurements. A comparison of curves *a* and *b* shows that the cooling of the sample and application of a bias voltage produce no qualitative changes in the Raman scattering, so that the low-temperature IETS results and the 300-K Raman results are comparable. In Fig. 12, we show the Raman spectrum of an Ag tunnel junction laid down on 1600 Å of CaF₂ and doped with benzoic acid, and the Raman spectrum of benzoic acid. These spectra were obtained using 6471-Å light. The preceding spectra establish the validity of our comparisons of the SER and IETS spectra and also show that not all dopants in our tunnel junctions have enhancement factors large enough to produce observable spectra.

Figure 4 showed that the SER spectrum is more than just an amplified version of the normal Ra-

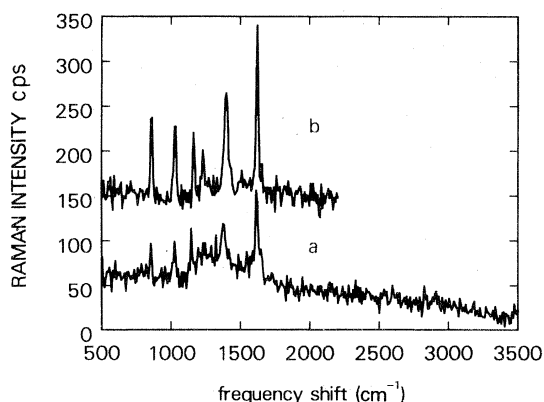


FIG. 11. *a*, the 300-K surface-enhanced Raman spectrum of 4-pyridine carboxylic acid in an Al-AIO_x-Ag tunnel junction laid down on CaF₂. *b*, the surface-enhanced Raman spectrum of 4-pyridine carboxylic acid in an Al-AIO_x-Ag tunnel junction on CaF₂. This spectrum was measured at 2 K with the junction biased at 0.5 V. Both *a* and *b* were excited by 5308-Å light.

man spectrum. Not all of the Raman lines are enhanced by the same amount. In Table I, we list several of the strongest Raman lines of 4-pyridine carboxylic acid as tabulated by Green and Harrison⁴⁹ together with their assignments and their relative strengths. We also list in this table the relative intensities of the corresponding lines observed in the tunneling spectrum of our pyridine carboxylic acid-doped Ag junctions. Also listed in this row is the 1380-cm⁻¹ COO vibration. We complete the table by listing the corresponding SER lines of the molecule in the Ag tunnel junction with their relative intensities. The interaction of the molecule and the metal surface does not produce any substantial shifts in the vibrational frequencies of the observable lines. This is similar to what has been observed in IETS studies.³² The enhancement factors show a variation of at least 2 orders of magnitude for different lines. The variation in the enhancement factor could be considerably greater and is limited by the experimental sensitivity. Table I also shows that lines with the same symmetry (for example ν_2 and ν_7) have enhancement factors that can vary by more than a factor of 100. This means that the differences in the enhancement factors for different lines cannot be associated with the selection rules for Raman scattering from the vibration. Similar behavior was observed for other dopants such as nitrobenzoic acid and acetylbenzoic acid. These results suggest that SER scattering involves more than just the modulation of the molecular polarizability.

The SER scattering from the benzoic acid-doped sample (Fig. 12) is barely observable. The IETS spectrum of this sample shows the

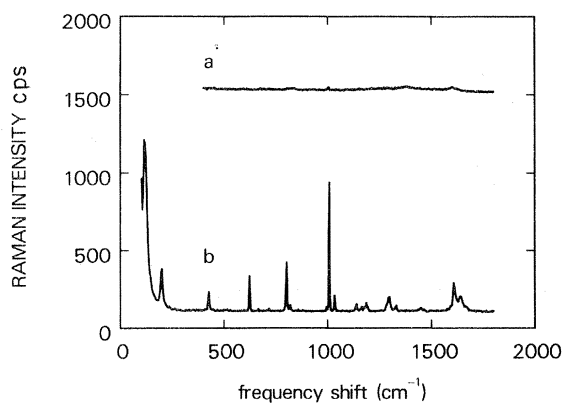


FIG. 12. *a*, the surface-enhanced Raman spectrum of benzoic acid in an Al-AIO_x-Ag tunnel junction laid down on 1200 Å of CaF₂. *b*, the Raman spectrum of a benzoic acid pellet. The spectra were excited by the 6471-Å line of a Kr laser.

TABLE I. Some vibrational modes of 4-pyridine carboxylic acid. Several of the principle vibrational Raman lines of 4-pyridine carboxylic acid with their symmetries, assignments, and relative strengths (Ref. 49). The relative intensities of the corresponding lines and the 1380-cm^{-1} COO mode as seen in IETS measurements on Al-AlO_x-Ag tunnel junctions doped with this molecule. The relative intensities and energies of these lines as seen in SER scattering from such a tunnel junction fabricated on a diffraction grating.

Bulk (cm ⁻¹)	Assignment	IETS intensity	SER (cm ⁻¹)	Intensity
3061	<i>a</i> ¹ , $\nu_2(\text{CH})$, 1.1	0.1		<0.01
1711	<i>a</i> ¹ , $\nu_6(\text{CO})$, 0.4	<0.01		<0.1
1594	<i>a</i> ¹ , $\nu_7(\text{CC})$, 1.0	1.0	1610	1.0
		0.33	1380	0.6
1190	<i>a</i> ¹ , $\nu_{15}(\text{CH})$, 0.8	0.13	1210	0.15
		0.1	1160	0.33
991	<i>a</i> ¹ , $\nu_{18}(\text{ring})$, 2.7	0.12	1014	0.4

chemisorbed benzoic acid. Therefore, the enhancement factor for benzoic acid under Ag is at least 20 times smaller than that of nitrobenzoic acid or 4-pyridine carboxylic acid. A similar result was obtained by Burstein, Chen, and Lundquist⁹ in their experiments with discontinuous films laid down on chemisorbed monolayers of benzoic acid. Because these experiments were all performed on different samples and given our ignorance of how the Ag counterelectrode forms on the molecular monolayer, the results cannot be interpreted in a simple manner. However, we have also studied Ag junctions doped with mixtures of benzoic acid and nitrobenzoic acid. In Fig. 13, we show the Raman spectra obtained from Al-AlO_x-Ag junctions laid

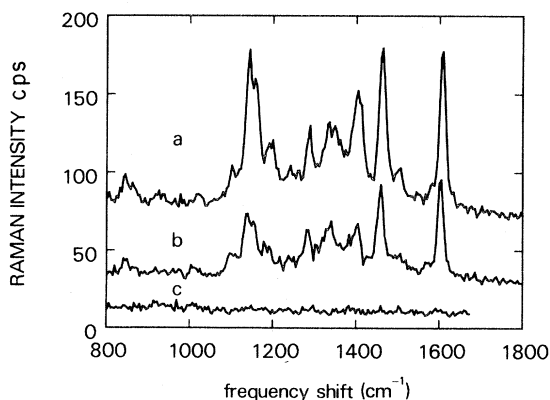


FIG. 13. Surface-enhanced Raman spectrum of Al-AlO_x-Ag junctions doped with mixtures of nitrobenzoic acid and benzoic acid and laid down on 1200 \AA of CaF₂. *a*, 100% nitrobenzoic acid. *b*, 1:3 mixture of nitrobenzoic acid and benzoic acid. *c*, 100% benzoic acid.

down on 1600 \AA of CaF₂ and doped with nitrobenzoic acid, a 1:3 mixture of nitrobenzoic acid and benzoic acid, and pure benzoic acid. The intensity of the nitrobenzoic acid spectra decreases as expected, with decreasing nitrobenzoic acid concentration but no significant Raman scattering from the benzoic acid is ever observed.

Figure 13 rules out the possibility that there is a chemical interaction between the nitrobenzoic acid and Ag producing a special surface morphology that would give an extra enhancement for the nitrobenzoic acid-doped junctions but not for the benzoic acid-doped junctions. The variation of the intensity of the nitrobenzoic acid scattering with nitrobenzoic acid concentration and radiotracer studied on other codoped systems show that both species are present in the junction. The failure to observe any effects of molecule-molecule interactions in IETS studies suggest that the molecules are randomly distributed on the surface.⁵⁰ Any field enhancement seen by the nitrobenzoic acid molecules will be seen by the benzoic acid molecules. The failure to observe scattering from the benzoic acid molecules in the 1:3 mixture shows that the interaction responsible for the molecule and vibrational mode dependence of the enhancement of the Raman scattering efficiency is not only molecule specific but also local.

Such an additional contribution to the SER intensity can arise from (1) the presence of submicroscopic roughness producing enhanced electromagnetic fields associated with localized plasmon resonances,^{21,51} (2) the polarization of the metal by the molecule as treated in the image-charge approxima-

tion,^{24,25} and (3) the modulation of the conduction-electron density at the metal surface by the electronic structure of the molecule.^{19,26}

Our Ag-molecule interfaces must be rough on the atomic scale, given their method of preparation. Chen *et al.*⁵² have experimentally shown that the electromagnetic fields above an anodized Ag surface, similar to those used in SER experiments in electrolytic cells, can be enhanced by an order of magnitude, producing possible enhancements of the Raman intensity of 4 orders of magnitude. If the roughness features on these surfaces could be modeled by 50 Å or smaller bumps,¹⁸ then the field enhancements would decay over a distance comparable to the thickness of a monolayer.⁵¹ However, comparisons of the optical properties of tunnel junctions laid down on gratings with tunnel junctions laid down on 1600-Å-thick layers of CaF₂ evaporated on a grating surface suggest that our grating surfaces are still reasonably smooth. They do not have the dark appearance of the heavily anodized surfaces. For example, the continuum optical emission⁴⁰ from the deliberately roughened tunnel junctions laid down on thick CaF₂ is almost 2 orders of magnitude stronger than the continuum emission from the biased tunnel junctions on the unroughened gratings. The gratings emission is of course dominated by the SPP emission.³⁶ The continuum emission is due to the excitation of localized plasmon resonances⁵³ which have been shown to produce SER scattering on discontinuous films. These results suggest that the Raman enhancement associated with the localized resonances on our grating surfaces will be considerably smaller (at least 100 times) than those on the deliberately roughened surfaces. Since we require an additional enhancement of the order of 3 orders of magnitude or more, this additional field enhancement will probably not be able to completely explain our experimental results. Furthermore, it does not appear that it can readily explain the molecule and mode-dependent results we observe. If two modes have the same symmetry, they should show the same enhancement, and we have seen in Table I that this is apparently not the case. While it is possible that the overall Raman intensities may be determined by a combination of localized and delocalized conduction-electron resonance, this combination cannot explain the appearance of the experimentally observed spectra, in particular the variation in the relative intensities of different lines.

Both the polarization of the metal surface by the

molecule via the image-charge model and the modulation of the conduction-electron density at the metal surface by the molecular vibrations can produce Raman tensors different from those produced by the normal modulation of the molecular polarizability by the molecular vibrations.^{19,24}

While both models are unlikely to produce the giant enhancements necessary to explain the surface Raman effect by themselves, when combined with the enhanced fields of the plasmon resonances,^{19,25} they can result in enhancements close to those observed. However, the enhancement obtained from the image model is strongly dependent on the exact position of the molecule with respect to the image plane of the surface. At the atomic scale, the position of the image plane will depend on the surface topology. If the surface were treated as a collection of 50-Å spheres, then the image plane for an adsorbed molecule will not be the classical image plane obtained from treating the surface as a flat plane. In fact, the enhancement due to the image model is substantially reduced for a small sphere.⁵⁴

There are two distinct correlations between the IETS spectra of our Ag junctions and the SER spectra. In Fig. 14, we compare the IETS spectra of a benzoic acid-doped Al-AlO_x-Pb junction and a 4-pyridine carboxylic acid-doped Al-AlO_x-Ag junction. The high-energy 3061-cm⁻¹ C-H vibra-

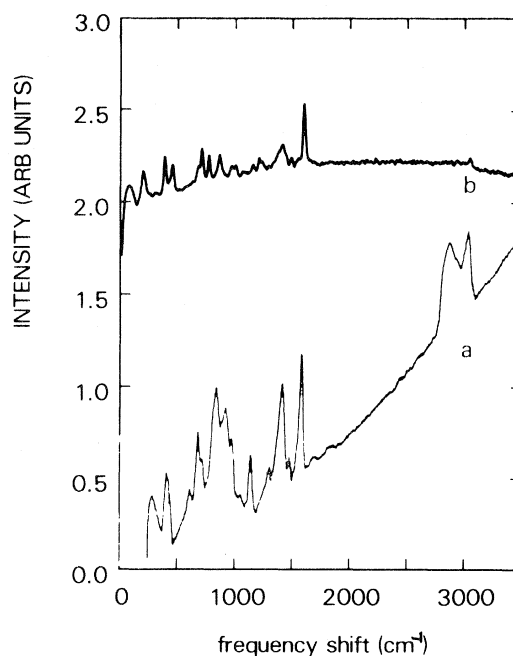


FIG. 14. IETS spectra of *a*, a benzoic acid-doped Al-AlO_x-Pb tunnel junction and *b*, a 4-pyridine carboxylic acid-doped Al-AlO_x-Ag tunnel junction.

tion is clearly seen in the Pb junction but is extremely weak, though still sharp and well defined in the Ag junction. The elastic tunneling background which rises monotonically with increasing bias voltage in the Pb junction shows a broad maximum in the Ag case and decreases with increasing bias voltage for biases above 3000 cm^{-1} ($> 0.40 \text{ eV}$). The weak high-energy peaks and the anomalous elastic scattering background have been correlated by Korman *et al.*³³ with tunnel junction structures where Φ_{b2} (Fig. 1) is less than 1 eV. The monotonically increasing elastic scattering background and strong CH vibrations are characteristic of barrier heights above 2.0 eV. Lau and Coleman³³ have reported that the effective barrier heights for Ag junctions are relatively low, often of the order of 1 eV or less.

We find from Table I that the intensity pattern of the SER spectrum does not show any significant resemblance to the intensity pattern of the Raman scattering from the molecule in the bulk. These changes are not associated with the chemisorption of the molecule on the oxide but rather with the presence of the Ag overlayer.³⁸ They suggest that the mechanisms responsible for SER scattering and normal Raman scattering are different. While not all the lines observed in IETS are seen in the SER scattering, the relative intensities of the SER active lines are comparable in both the SER and the IETS spectra. This can be seen most clearly if we consider the 1014- and 1610-cm^{-1} carbon ring modes, the 1380-cm^{-1} COO stretch mode, and the 3061-cm^{-1} C-H stretch mode.

These results suggest a connection between the processes responsible for IETS from molecular vibrations in these tunnel junctions and SER scattering. Any contribution to Raman scattering from the tunneling interaction would be short ranged and limited to the first molecular monolayer. It would involve a polarizability tensor distinct from

the normal Raman polarizability tensor. Jha *et al.*¹⁹ have recently considered the modulation of the optical polarizability of a metal surface by the vibrations of an adsorbed molecule when Φ_{b2} is relatively low. They showed that this could produce a significant new channel for adsorbate Raman scattering.

In Table II, we show the dependence on Φ_{b2} and d_2 (Fig. 1) of the magnitude of the Raman tensor associated with the scattering process considered by Jha *et al.* The details of the theoretical treatment responsible for Table II are in Ref. 19. The results in Table II are normalized against an average Raman polarizability of $Z_{\text{eff}} a_0^2$ where Z_{eff} is the effective molecular charge and a_0 is the Bohr radius. From Korman *et al.*,³³ Φ_{b2} can vary from less than 1 eV to as large as 5–6 eV. For all values of Φ_{b2} , the modulated surface polarizability contribution to the Raman tensor will be negligible if d is greater than 10 Å. This is expected since tunneling lengths are of the order of an atomic distance. However, for low values of Φ_{b2} , the modulation of the surface polarizability by the molecules can produce an effective Raman tensor considerably larger than the normal Raman tensor. Experimental values for the Raman polarizability vary from between 0.05 and 10 \AA^2 for nonresonant Raman scattering.⁵⁵ The Raman scattering cross section $d\sigma/d\Omega$ is related to the modulated surface polarizability $d\beta/dR_j$ through the relationship

$$\frac{d\sigma}{d\Omega} = \frac{(2\pi)^4}{\lambda^4} \left[\sum_{j=0}^n \left[\frac{d\beta}{dR_j} \right] dR_j \right]^2 \quad (4)$$

From Table II, for a molecule to image plane distance of 2.5 \AA and $\Phi_{b2} = 0.50 \text{ eV}$, the Raman polarizability due to the modulation by a single vibrating atom of the electrons tunneling out of the metal surface can be 150 \AA^2 . Values of $d\beta/dR_j$ of this magnitude will result in a Raman cross section

TABLE II. The dependence of the normalized surface Raman polarizability $d\beta/dR_j$ on both the molecule metal distance d_2 and the molecule metal barrier height Φ_{b2} . The surface Raman polarizability is normalized against $Z_{\text{eff}} a_0^2$ where a_0 is the Bohr radius and $Z_{\text{eff}} = 1$ or a Raman polarizability of 0.25 \AA^2 .

d_2 (Å)	Φ_{b2} (eV)		
	0.5	1.0	1.5
1	1986	155	31
2.5	597	22	2.5
5.0	41	0.37	0.015
10	0.016	0.00034	0.000025

of the order of 10^{-28} cm², or 3 orders of magnitude larger than the nominal Raman cross section of 10^{-31} cm². When combined with the SPP field enhancement considered previously, it produces a net enhancement of 5 orders of magnitude.

Any calculation of a Raman cross section involves many parameters. The calculation of Jha *et al.*¹⁹ is based on the optical conductivity of Ag and on parameters deduced from the IETS of the junctions. On the basis of the work of Korman *et al.*³³ and the IETS results from our junctions, Φ_{b2} 's for the doped junctions which show strong SER scattering are 1 eV or less.

The theoretical predictions of the magnitude of the Raman cross section due to the modulation of the electrons tunneling out of the metal are subject to uncertainty since neither the correct normal modes of the molecule or the actual electronic wave functions of the molecule have been considered. However, we can compare the qualitative predictions of the model with our experimental results.

The principal feature of the model of Jha *et al.*¹⁹ is a short-range, molecule-specific enhancement of I_s . This is what was observed when we considered the SER spectra of codoped tunnel junctions. Because the enhanced Raman scattering arises from the molecular modulation of the surface polarizability of the metal, and not from the modulation of the molecular polarizability, the SER spectrum can appear quite different from the normal bulk Raman spectrum. This is shown in Table I when we compare the intensity patterns for the SER and normal Raman spectra. The similarities in our theoretical treatment¹⁹ of SER scattering and the theoretical treatment of IETS (Refs. 32 and 33) suggest the relative intensity patterns of the SER and IETS spectra of identically doped tunnel junctions should be similar. This is the case if we consider the principal lines of the SER spectrum. However, not all the lines seen in the IETS spectra are observed in the Raman scattering. Within our model, it would be surprising if the SER spectra completely agrees with the IETS spectra, since there are substantial differences in the physical processes. For example, in the IETS theory, the scattering matrix element connects two tunneling wave functions which enter the barrier region from the opposite sides of the barrier. In the SER theory, the electronic wave functions which are scattered by the molecular vibration all come from one side of the junction.

The model of Jha *et al.*¹⁹ predicts the angular

distribution and polarization of the scattered light for values of θ_s away from the SPP resonance angles. The scattered radiation arises from oscillating dipoles oriented normal to the surface of the metal. There will be no dipole scattering for $\theta_s=0$. The scattered light for other values of θ_s should be *p* polarized. This is not observed in our measurements of SER scattering from tunnel junctions fabricated on a grating. However, the directions of the radiating surface dipoles are determined by the local normals on our films. At the atomic level, our evaporated films on developed photoresist surfaces will be neither smooth nor flat. The evaporation of the Ag film on the molecular monolayer raises questions as to the definition of the atomic surface plane at the molecule-metal interface. While the scattered field due to the modulated surface dipole is zero in the direction of the local normal at the surface, the variation of the local normals about the macroscopic plane of the grating will produce enhanced scattering at $\theta_s=0$. Furthermore, theoretical calculations by Kirtley *et al.*⁵⁶ for the IETS cross section of adsorbates find that the electron molecule interaction can involve the higher-order multipoles of the molecule. The modulation of the surface charge distribution by the higher-order multipole interaction will produce scattering at $\theta_s=0^\circ$.

VI. SUMMARY

We have used doped, inelastic electron tunneling spectroscopy junctions as a model system to study the phenomena of surface-enhanced Raman scattering. We have made use of both the fact that evaporated thin films conform to the topology of the substrate and of our ability to fabricate grating profiles in our substrates in order to create systems with easily characterized surface topologies to isolate the effects of microscopic (100–10 000 Å) surface roughness on SER scattering. The coupling of light to the surface electromagnetic waves of an Ag substrate can produce an enhancement of 2–3 order of magnitude of the Raman scattering efficiency for adsorbed molecules. The coupling of the scattered fields of the molecules to the radiative surface electromagnetic waves of the substrate can provide a further enhancement of the Raman scattering efficiency. These results suggest that surface-enhanced Raman scattering arises from the enhancement of the electromagnetic fields on a rough Ag surface. However, a second set of re-

sults show there is also a local, short-range molecule-specific contribution to SER scattering. This mechanism will depend strongly on the exact details of the interaction between the molecule and the metal. We have modeled this effect using a simple barrier between the molecule and the metal and find that strong enhancements correspond to barrier heights of 1 eV or less. Our model represents the simplest possible description of the interaction between the electronic structure of the molecule and the metal surface. The total surface-enhanced Raman effect will be the product of both the short- and the long-range effects.

Our experimental results are consistent with experimental results obtained on other systems used for studies of surface-enhanced Raman scattering. Experiments in ultrahigh vacuum and on colloids in solution show the effect of the excitation of the surface electromagnetic wave resonances and the presence of a short-range, molecular-mode-independent contribution to the Raman enhancement.

These results show that the observation of surface-enhanced Raman scattering depends on a number of factors. Although the enhancement of the Raman efficiency due to the excitation of the surface electromagnetic modes of Ag or other noble metals is generally less than 10^3 for the grating structures, somewhat larger enhancements can be obtained if alternative structure can be fabricated.¹⁴ These include arrays of ellipsoids where the resonant excitation of the surface electromagnetic modes by the Raman-scattered fields of the molecule can produce an additional enhancement com-

parable to the enhancement of the incident field at the molecule. In this case, the enhanced scattering will involve both the first monolayer and subsequent layers.

The enhancement of the Raman scattering due to the tunneling interaction of the adsorbate and the electrons of the metal can depend on the electronic wave functions. In our experiments, the local effects on the Raman scattering efficiency produce variations in the Raman cross section of between 2 and 3 orders of magnitude. Experiments in ultra-high vacuum on clean surfaces prepared at room temperature or by sputtering at low temperature result in first layer enhancements that are between 30 and 500 times larger than the enhancement for a more distant layer.^{4,13} Experiments on low-temperature evaporated films produce first layer enhancements that can be 4 or more orders of magnitude larger than any enhancement of a second layer.^{5,6,9} These differences may reflect differences in the atomic structure of the surface which can have a significant effect on the electronic structure of the adsorbate.⁵⁷

ACKNOWLEDGMENTS

We thank Professor E. Burstein and Dr. Frank Stern for many helpful discussions, Mr. J. A. Bradley, M. T. Prikas, and A. M. Torressen for invaluable experimental assistance, and C. Aliotta for electron micrographs of our samples.

*Present address: Tata Institute of Fundamental Research, Bombay, India.

¹M. Fleischmann, P. J. Hendra, and A. J. McQuilla, *Chem. Phys. Lett.* **26**, 163 (1974). There are a number of review articles on the subject of SER scattering. Several can be found in the collection, *Surface-Enhanced Raman Scattering*, edited by R. K. Chang and T. E. Furtak (Plenum, New York, 1982).

²D. L. Jeanmaire and R. P. van Duyne, *J. Electroanal. Chem.* **84**, 1 (1977).

³M. G. Albrecht, J. A. Creighton, R. E. Hester, and J. A. D. Matthew, *Chem. Phys. Lett.* **55**, 55 (1978); T. Furtak, *Solid State Commun.* **28**, 903 (1978); B. Pettinger and U. Wenning, *Chem. Phys. Lett.* **52**, 253 (1978).

⁴R. R. Smardzewski, R. J. Colton, and J. S. Murdey, *Chem. Phys. Lett.* **68**, 53 (1979); G. R. Eesley, *Phys. Lett.* **81**, 193 (1981); G. R. Eesley and D. L. Simon,

J. Vac. Sci. Technol. **18**, 629 (1981).

⁵T. H. Wood and M. V. Klein, *J. Vac. Sci. Technol.* **16**, 459 (1979); I. Pockrand and A. Otto, *Solid State Commun.* **35**, 861 (1980); T. A. Wood, M. V. Klein, and D. A. Zwemer, *Surf. Sci.* **107**, 625 (1981).

⁶M. Moskovits and D. P. DiLella, *Chem. Phys. Lett.* **73**, 500 (1980); M. Moskovits and D. P. DiLella, *J. Chem. Phys.* **73**, 6068 (1981).

⁷J. M. Rowe, C. V. Shank, D. A. Zwemer, and C. A. Murray, *Phys. Rev. Lett.* **44**, 1770 (1980).

⁸E. Burstein, C. Y. Chen, and S. Lundquist, in *Proceedings of the US-USSR Symposium on Light Scattering*, edited by J. L. Birman, H. Z. Cummins, and K. K. Rebane (Plenum, New York, 1980), pg. 479.

⁹H. Seki and M. Philpott, *J. Chem. Phys.* **73**, 5376 (1980).

¹⁰J. A. Creighton, C. G. Blatchford, and M. G. Albrecht, *J. Chem. Soc. Faraday Trans. 2* **75**, 790

- (1979); M. E. Lippitsch, *Chem. Phys. Lett.* **74**, 125 (1980); H. Wetzel and H. Gerischer, *ibid.* **76**, 460 (1980); M. Kerker, O. Siiman, L. A. Bumm, and D. S. Wang, *Appl. Opt.* **19**, 3253 (1980); D. A. Weitz, T. J. Gramila, A. Z. Genack, and J. I. Gersten, *Phys. Rev. Lett.* **45**, 355 (1980); K. U. Von Raben, R. K. Chang, and B. L. Laube, *Chem. Phys. Lett.* **79**, 465 (1981).
- ¹¹J. C. Tsang and J. R. Kirtley, *Solid State Commun.* **30**, 617 (1980); J. C. Tsang, J. R. Kirtley, and J. A. Bradley, *Phys. Rev. Lett.* **43**, 772 (1979).
- ¹²C. A. Murray, D. L. Allara, and M. Rhinewine, *Phys. Rev. Lett.* **46**, 57 (1981).
- ¹³P. N. Sanda, J. M. Warlaumont, J. E. Demuth, J. C. Tsang, K. Christmann, and J. A. Bradley, *Phys. Rev. Lett.* **45**, 1519 (1980).
- ¹⁴P. F. Liao, J. G. Bergmann, D. S. Chemla, A. Wokaun, J. Melngailis, A. M. Hawryluk, and N. P. Economou, *Chem. Phys. Lett.* **82**, 355 (1981).
- ¹⁵Y. Y. Teng and E. A. Stern, *Phys. Rev. Lett.* **19**, 511 (1967); D. L. Beaglehole and O. Hunderi, *Phys. Rev. B* **2**, 321 (1972).
- ¹⁶Y. J. Chen, W. P. Chen, and E. Burstein, *Phys. Rev. Lett.* **36**, 1207 (1976).
- ¹⁷M. Moskovits, *J. Chem. Phys.* **69**, 4159 (1978).
- ¹⁸D. S. Wang, M. Kerker, and H. Chew, *Appl. Optics* **19**, 2315 (1980); D. S. Wang and M. Kerker, *Phys. Rev. B* **24**, 1777 (1981).
- ¹⁹J. R. Kirtley, S. S. Jha, and J. C. Tsang, *Solid State Commun.* **35**, 509 (1980); S. S. Jha, J. R. Kirtley, and J. C. Tsang, *Phys. Rev. B* **22**, 3973 (1980).
- ²⁰B. Pettinger, A. Tadjeddine, and D. M. Kolb, *Chem. Phys. Lett.* **66**, 544 (1979); R. Dornhaus, R. E. Brenner, R. K. Chang, and I. Chabay, *Surf. Sci.* **101**, 367 (1980).
- ²¹C. Y. Chen and E. Burstein, *Phys. Rev. Lett.* **45**, 1287 (1980); J. Gersten and A. Nitzan, *J. Chem. Phys.* **73**, 3023 (1980); S. L. McCall, P. M. Platzman, and P. A. Wolff, *Phys. Lett.* **77A**, 381 (1980).
- ²²P. K. Aravind and H. Metiu, *Chem. Phys. Lett.* **74**, 301 (1980); P. K. Aravind, E. Hood, and H. Metiu, *Surf. Sci.* **109**, 95 (1981).
- ²³J. C. Tsang, J. R. Kirtley, and T. N. Theis, *Solid State Commun.* **35**, 667 (1980).
- ²⁴F. W. King, R. P. Van Duyne, and G. C. Schatz, *J. Chem. Phys.* **69**, 4472 (1978); S. Efrima and H. Metiu, *ibid.* **70**, 1602 (1979); **70**, 1939 (1979); P. J. Feibelman, *Phys. Rev. B* **22**, 3654 (1980); P. R. Hilton and D. W. Oxtoby, *J. Chem. Phys.* **72**, 6346 (1980).
- ²⁵W. H. Weber and G. W. Ford, *Phys. Rev. Lett.* **44**, 1774 (1980); G. W. Ford and W. H. Weber, *Surf. Sci.* **109**, 451 (1981); G. C. Schatz, M. Janik-Czachor, and R. P. van Duyne, *ibid.* **104**, 419 (1981).
- ²⁶A. Otto, *Surf. Sci.* **92**, 145 (1980); J. L. Gersten, R. L. Birke, and J. R. Lombardi, *Phys. Rev. Lett.* **43**, 147 (1979); S. L. McCall and P. M. Platzman, *Phys. Rev. B* **22**, 1660 (1980); J. K. Sass, H. Neff, M. Moscovits, and S. Holloway, *J. Chem. Phys.* **85**, 621 (1981); T. K. Lee and J. L. Birman, *Phys. Rev. B* **22**, 5961 (1980); B. N. J. Person, *Chem. Phys. Lett.* **82**, 561 (1981).
- ²⁷D. Heitmann, *Optics Commun.* **20**, 292 (1977).
- ²⁸E. Economou, *Phys. Rev.* **182**, 539 (1969).
- ²⁹P. B. Johnson and R. W. Christy, *Phys. Rev. B* **6**, 4370 (1973); C. J. Powell, *J. Opt. Soc. Am.* **72**, 84 (1970).
- ³⁰M. Dujardin and M. Theye, *J. Phys. Chem. Solids* **32**, 2033 (1971).
- ³¹B. Laks and D. L. Mills, *Phys. Rev. B* **20**, 4962 (1979).
- ³²P. Hansma and J. R. Kirtley, *Acc. Chem. Res.* **11**, 440 (1978); John Kirtley and P. K. Hansma, *Phys. Rev. B* **13**, 2910 (1976); J. Klein, A. Leger, M. Belin, D. Defourneau, and M. J. L. Sangster, *ibid.* **7**, 2336 (1973).
- ³³C. S. Korman, J. C. Lau, A. M. Johnson, and R. V. Coleman, *Phys. Rev. B* **19**, 994 (1979); J. C. Lau and R. V. Coleman, *ibid.* **24**, 2985 (1981).
- ³⁴J. M. Endriz and W. E. Spicer, *Phys. Rev. B* **4**, 4159 (1972).
- ³⁵I. Pockrand, *Phys. Lett.* **49A**, 259 (1974).
- ³⁶J. R. Kirtley, T. N. Theis, and J. C. Tsang, *Appl. Phys. Lett.* **37**, 435 (1980); J. R. Kirtley, T. N. Theis, and J. C. Tsang, *Phys. Rev. B* **24**, 5650 (1981).
- ³⁷J. D. Langan and P. Hansma, *Surf. Sci.* **52**, 211 (1975).
- ³⁸A. E. T. Kuiper, J. Medema, and J. J. G. M. van Bokhoven, *J. Catal.* **29**, 40 (1973).
- ³⁹B. Pettinger, U. Wenning, and D. M. Kolb, *Ber. Bunsenges. Phys. Chem.* **82**, 1326 (1978).
- ⁴⁰J. Lambe and S. L. McCarthy, *Phys. Rev. Lett.* **37**, 923 (1976).
- ⁴¹S. L. McCarthy and J. Lambe, *Appl. Phys. Lett.* **30**, 427 (1977).
- ⁴²W. H. Weber and G. W. Ford, *Opt. Lett.* **6**, 122 (1981).
- ⁴³R. F. Millar, *Proc. Cambridge Philos. Soc.* **69**, 217 (1971).
- ⁴⁴R. Petit, in *Electromagnetic Theory of Gratings*, edited by R. Petit (Springer, Berlin, 1980), p. 1.
- ⁴⁵D. Heitmann, *J. Phys. C* **10**, 397 (1977).
- ⁴⁶T. Furtak and R. Kester, *Phys. Rev. Lett.* **45**, 1652 (1980).
- ⁴⁷R. Dornhaus, M. B. Long, R. E. Brenner, and R. K. Chang, *Surf. Sci.* **93**, 240 (1980).
- ⁴⁸G. R. Erdheim, R. L. Birke, and J. R. Lombardi, *Chem. Phys. Lett.* **69**, 495 (1980).
- ⁴⁹J. H. S. Green and D. J. Harrison, *Spectrochim. Acta Part A* **33**, 75 (1977).
- ⁵⁰A. Cederberg, *Surf. Sci.* **103**, 148 (1981).
- ⁵¹T. H. Wood, D. A. Zwemer, C. V. Shank, and J. E. Rowe, *Chem. Phys. Lett.* **82**, 5 (1981).
- ⁵²C. Chen, A. R. B. deCastro, Y. R. Shen, and F. deMartini, *Phys. Rev. Lett.* **46**, 145 (1981).
- ⁵³R. W. Rendell, D. J. Scalapino, and B. Muhlschlegel, *Phys. Rev. Lett.* **41**, 1746 (1978).
- ⁵⁴G. S. Agarwal, S. S. Jha, and J. C. Tsang, *Phys. B* **25**

2089 (1982).

⁵⁵G. Varsanyi, *Vibrational Spectra of Benzene Derivatives* (Academic, New York, 1969).

⁵⁶J. R. Kirtley, D. J. Scalapino, and P. K. Hansma,

Phys. Rev. B 14, 3177 (1976).

⁵⁷J. Billman, G. Kovacs, and A. Otto, Surf. Sci. 92, 453 (1979).

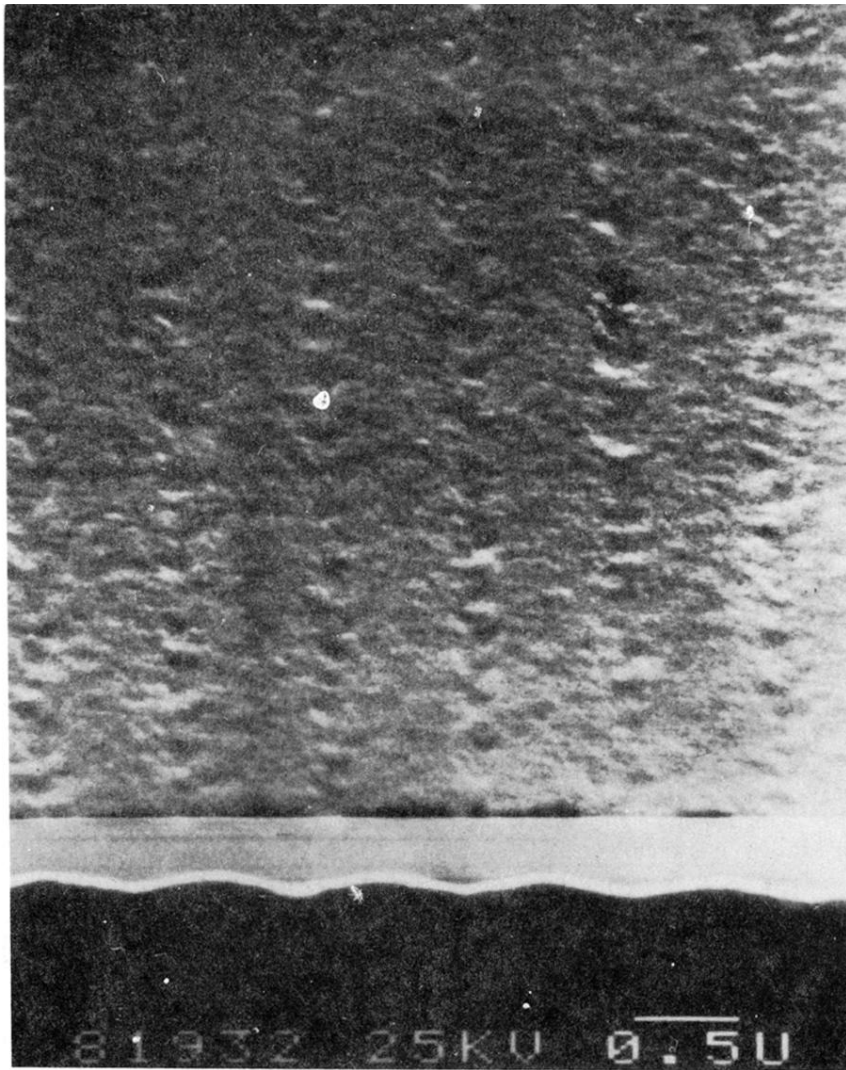


FIG. 2. Electron micrograph of an Al-AlO_x-Ag tunnel junction laid down on a holographic diffraction pattern developed in photoresist. Top is at normal incidence. White line at bottom is junction in profile.